*Bull. Mater. Sci.* (2022) 45:195
https://doi.org/10.1007/s12034-022-02764-8



# Morphological, linear and nonlinear optical characteristics of PVA/Ac–PVP blend filled with nanoparticles of titania

**G VEENA and B LOBO***
Department of Physics, Karnatak University's Karnatak Science College, Dharwad 580001, India
*Author for correspondence (blaise.lobo@gmail.com)

MS received 20 December 2021; accepted 26 May 2022

**Abstract.** Titanium dioxide ($TiO_2$) nanoparticle (NP)-filled poly(vinyl alcohol-co-acetate) [PVA/Ac]–polyvinyl pyrrolidone (PVP) blend composite films were prepared with filler level (FL) ranging from 0.0 to 4.89 wt% by solution casting technique. Scanning electron microscope images showed the uniform distribution of the nanofiller (NF) at low FL and the aggregation of the filler at higher FLs. Energy dispersive X-ray spectrometry was used to determine the elemental constituents present in the composite samples. The ultra violet–visible spectral data of the prepared composite films, obtained in the wavelength range of 190–1000 nm, were exploited to investigate the linear and nonlinear optical properties. The incorporation of $TiO_2$ NPs in PVA/Ac–PVP blend resulted in decrease of the optical bandgap. The type of transition was found to be indirect allowed transition in k-space. The values of linear optical parameters, including absorption coefficient ($\alpha$), refractive index ($n$), real ($\varepsilon_1$) and imaginary ($\varepsilon_2$) parts of dielectric constants of the composite films increased with increase in FL. Wemple and Didomenico method was used to determine the dispersion parameters. The value of high energy dielectric constant ($\varepsilon_\infty$) extracted from two different methods were in good agreement with each other and were found to vary as a function of FL. Linear optical susceptibility ($\chi^{(1)}$) and nonlinear optical parameters such as nonlinear refractive index ($n_2$) and third-order nonlinear optical susceptibility ($\chi^{(3)}$) were enhanced due to the incorporation of the $TiO_2$ NPs in PVA/Ac–PVP. Sample with FL of 4.89 wt% exhibited a maximum $n_2$ value of 50389.1 $\times$ $10^{-17}$ esu, while for pure PVA/Ac–PVP blend, it was 1.3 $\times$ $10^{-17}$ esu. Thus, it can be seen that the incorporation of $TiO_2$ NPs has enhanced the optical properties of the resulting composite, and this material can be considered as a promising material for flexible optoelectronic applications.

**Keywords.** PVA/Ac–PVP blend; $TiO_2$ NP; SEM; EDS; linear and nonlinear optical properties.

## 1. Introduction

Synthesis of new polymeric composite materials and the study of their electrical and optical properties have been the focus of contemporary research in material science. This is due to the suitability of these composites to be utilized in various applications, including electrochemical cells, fuel cells, supercapacitor and batteries [1–5]. The interesting optical properties exhibited by the new composite materials are explored in order to utilize them in the fabrication of optical devices like sensors and light-emitting diodes (LEDs). The optical characterization of a polymeric composite material includes the use of techniques such as UV–visible absorption, Raman spectroscopy studies and photoluminescence studies, which are helpful to elucidate the electronic properties of the material [6–9]. UV-Visible spectroscopy is based on the electronic transitions taking place between the highest occupied molecular orbital and lowest unoccupied molecular orbital of the material due to its interaction with electromagnetic radiation in the ultraviolet (UV) and visible regions of the electromagnetic spectrum. Incorporation of a suitable filler or/and blending of the polymer with some other polymer are some of the most popular and easiest methods which have been adopted in order to obtain a polymeric composite material with desired properties, for their use in optoelectronic applications [10–13]. It is to be noted that the changes in the optical properties exhibited by a particular polymeric composite material greatly depends on the type of additive which has been incorporated in the base polymeric material and its concentration (which can be used to tailor the properties accordingly). Additives/fillers are introduced into the polymer matrix with a view to enhance the material properties, along with an intention to dilute the material with something that is cost effective. But, the incorporation of a nanofiller (NF) as an additive not only results in the improvement of one or more functional properties, but also renders the material useful for different applications [14–18]. The incorporation of a filler in the polymeric matrix could lead to changes in the chemical composition of the resulting material, which can be manifested as modifications in its optical properties due to the changes in the power of polarization, coordination number and the number of nonbonded

Published online: 05 October 2022

functional groups within the polymer matrix [19]. UV–visible spectroscopy is an important technique to determine the various optical parameters and also to study the interaction between the components (in the NF) incorporated in polymeric materials [20]. The optical absorption spectra show changes in the intensity and shifts in the absorption edge and the formation of new intermediate band/ bands due to optically induced transitions in noncrystalline and crystalline materials. This provides a better insight into the energy band structure of the new material, and thus helps to predict their applicability in certain areas, such as optoelectronics. The study of linear and nonlinear optical parameters (optical bandgap, linear and nonlinear refractive index and third-order nonlinear susceptibility) of these composites are crucial for exploring their potential applications [21–25].

Recently, the incorporation of inorganic NFs as additives in polymeric host materials has attracted significant scientific and technological interest. This is because, the incorporation of inorganic nanoparticles (NPs) in a polymer results in new and high-performance materials with enhanced optical, electrical, thermal and mechanical properties due to the combined effect of both inorganic (filler) and organic (polymer) components. Polymer composites with inorganic filler are greatly used in optical [26], magnetic [27–29], mechanical and biomedical applications [30,31]. Of all the inorganic NFs, semiconducting nanofillers (SN) have created extensive research interest. Some of the most frequently employed SN includes lead sulphide (PbS) [32], cadmium sulphide (CdS) [33], zinc oxide (ZnO) [34] and $TiO_2$ [35]. Of these, the fillers such as PbS, ZnO or $TiO_2$ in polymer matrix are popularly used as effective optical additives [26]. These materials are extensively studied for various optical applications, such as light absorption, photoluminescence, extreme refractive index, dichroism, electromagnetic wave absorption and electromagnetic interference shielding [36].

The use of inorganic semiconducting NPs such as ZnO and $TiO_2$ incorporated in polymeric materials as photoprotective materials (UV absorbers) are of great interest due to their photostability. Titanium dioxide ($TiO_2$) or titania, when used as filler, is a typical absorber of electromagnetic radiation, which selectively absorbs UV light and re-emits it at a less harmful wavelength, mainly in the form of heat [37]. $TiO_2$ NPs are effectively used for redox processes and also in photoelectrochemical cells [38]. $TiO_2$ NPs, due to their photocatalytic behaviour and low cost are widely used in environmentally relevant applications, such as air and water purification [39], and the degradation of the organic contaminants [40].

PVA/Ac–PVP blend is known for its versatile properties, which make it suitable for vital applications such as energy storage devices, drug delivery and tissue engineering. This blend exhibits excellent miscibility and water absorbing properties, when combined in the ratio of 1:1 [41]. The properties of PVA/Ac–PVP blend depends on the extent of miscibility of its components. Literature reveals that there is formation of thermodynamically miscible blends in almost all possible compositions of PVA/Ac and PVP, due to the interaction between the hydroxyl (OH) and carbonyl (C=O) groups of PVA/Ac and PVP, respectively [41]. The blending of PVA/Ac with PVP makes available more number of polar groups which are found in the side chains of the polymeric blend (which provides sites for the interaction of $Ti^{+}$ of the $TiO_2$ NPs with molecules of the polymeric blend) [42]. As a result of this interaction, interesting changes in the optical, thermal and electrical properties of the resulting composite can be expected; these properties can be tailored by varying the concentration of the titania NPs in the host polymeric blend [42]. PVA/Ac and PVP are chosen to be the components of polymeric blend matrix. This blend exhibits attractive properties, being water soluble, biodegradable and nontoxic. PVA/Ac is marked by its excellent charge storage capability. PVA/Ac when incorporated with different inorganic fillers, exhibits FL-dependent electrical and optical properties. This is due to the presence of OH groups on its side chains, which provide sites for interaction of the polymer molecules with the filler [43–45]. PVP usually exhibits low electrical conductivity, and therefore it is employed as a dielectric material for the fabrication of organic thin film transistor and other optoelectronic devices [46,47]. PVA/Ac–PVP blend filled with various NPs has been extensively studied for a wide variety of applications [48–51].

The authors have previously reported the results of spectroscopic, thermal, structural and electrical properties of this composite sample (PVA/Ac - PVP blend filled with titania NPs) elsewhere [42]. It is seen from the X-ray diffraction patterns of these composites that the amorphousness of the sample increased due to the incorporation of nano titania and the values of crystallite size were found to be in nano metre scale. Thermal analysis on this sample supported the XRD results by showing a decrease in the glass transition temperature and increase in the thermal stability of the samples with an increase in the FL. Fourier transform-infrared (FT-IR) spectra revealed the formation of a charge transfer complex (CTC) due to the interaction of NFs with the polar groups of the polymeric matrix. Spectroscopic studies also indicated the decrease in the amorphousness of the sample with the increase in FL. This increase in amorphousness of the composite sample, when compared to that of the pure sample, resulted in the enhancement of its electrical conductivity, as depicted by DC and AC electrical studies. The sample with 4.89 wt% of titania in PVA/Ac–PVP blend exhibited the highest conductivity of $8.63 \times 10^{-3}$ S $m^{-1}$ at 363 K. The major contribution to the electrical conductivity of these composite samples was found to be from ions as concluded from the results of the transference number determination. The aim of this study is to gain a comprehensive understanding of the optical properties of $TiO_2$ NP-filled PVA/Ac–PVP composites. This study focuses on the determination of different types of electron transitions (due to absorption of

UV–visible photons), along with linear and nonlinear optical properties of $TiO_2$ NP-incorporated PVA/Ac–PVP blend composites. Although literature reveals a significant amount of work in the field of inorganic salt-filled polymer composites for various applications, it is to be noted that the detailed study of optical properties of inorganic semiconducting NPs in polymer blend is limited. The use of inorganic semiconducting NPs such as $TiO_2$ in a polymeric blend such as PVA/Ac–PVP can be expected to result in a composite material with unique combination of material properties. A detailed study of the optical properties of these composite materials is helpful to understand their properties and the same can be exploited to design and fabricate materials for new and interesting applications, such as optoelectronic and magneto-optic applications.

## 2. Experimental

### 2.1 *Sample preparation*

Details regarding the preparation of $TiO_2$-filled PVA/Ac–PVP composites are given elsewhere [42]. For the sake of completeness, a few aspects are specified here. Solution casting technique was used to prepare $TiO_2$-filled PVA/Ac–PVP composites with filler level (FL) ranging from 0.01 up to 4.89 wt%. PVA/Ac and PVP were used as the components of the blend. Both partially hydrolysed PVA (PVA/Ac) and PVP were used as-received from HiMedia Laboratories Pvt. Ltd., Mumbai. Anatase $TiO_2$ NPs was used as the NF. Polymer blend was prepared by dissolving 2 g each of PVA/Ac and PVP in 100 ml of double-distilled water by constant stirring for 24 h. Appropriate amount of $TiO_2$ NP was dispersed in double-distilled water. This solution is later transferred into PVA/Ac–PVP aqueous blend in different volumes and stirred well. Later, $TiO_2$ NP dispersed PVA/Ac–PVP aqueous solution was poured into clean Petri dishes and kept in an air-cooled oven for the evaporation of water molecules. After drying, the films were peeled from the substrate and stored in a desiccator for further studies.

The FL is calculated using equation (1),

$$\mathrm{FL\,(wt\%)} = \frac{m_\mathrm{f} \times 100}{m_\mathrm{f} + m_\mathrm{p}}. \tag{1}$$

In equation (1), FL is the filler level, $m_\mathrm{p}$ is the mass of polymer (PVA/Ac–PVP) and $m_\mathrm{f}$ is the mass of filler.

### 2.2 *Methods*

Scanning electron microscope (SEM) images along with energy dispersive X-ray spectrometry (EDS) spectra for pure and $TiO_2$ NP-filled composites were obtained using Nova Nano SEM, a field-emission scanning electron microscope coupled with EDS instrumentation. Optical spectra have been recorded using Hitachi U 3310 UV-Vis-NIR spectrometer, in wavelength range varying from 190 up to 1000 nm, at 25°C.

## 3. Results and discussion

### 3.1 *SEM and EDS analysis*

The incorporation of $TiO_2$ NPs into the PVA/Ac–PVP blend has drastically affected the surface morphology of the material, which has been studied using SEM. The SEM images were obtained using Nova Nano SEM, a field emission scanning electron microscope coupled with EDAX instrumentation. EDAX spectra along with the SEM images (inset) for pure PVA/Ac–PVP blend and $TiO_2$-filled PVA/Ac–PVP blend composites are shown in figure 1. The SEM images of pure PVA/Ac–PVP blend reveals a homogeneous surface with no micro-structural or nano-structural features, which is in fact expected for the homogeneous blend of PVA/Ac and PVP. For the composites with FL of 0.01 wt%, a good dispersion of $TiO_2$ NPs in the polymer matrix is observed (spherical nano-structures); but, aggregation of $TiO_2$ NPs is seen at FL 0.36 wt%. This aggregation results in the formation of micro-structures at 0.89 wt% and finally, phase separation is observed at 4.90 wt%.

The incorporation of $TiO_2$ has helped to decrease the crystalline regions of the polymer blend and the degree of crystallinity is found to be lower in composite films at all FLs when compared to that of the pure blend. This is also manifested in the FT-IR analysis, which reveals a drastic reduction in the intensity of the absorption band at 1114 $cm^{-1}$ [42], which implies a decrease in the degree of crystallinity of the composite sample, when compared to the pure polymeric blend [42]. The incorporation of $TiO_2$ leads to an enhancement of thermal, optical and electrical properties [42] of PVA/Ac–PVP blend. The analysis of EDS spectra reveal the elemental constituents present in these samples.

Figure 1 represents the EDS spectra for pure and $TiO_2$ NP-filled PVA/Ac–PVP blend composites. EDS peak assignments of pure and $TiO_2$ NPs-filled PVA/Ac–PVP blend composites are tabulated in table 1. The EDS scans of PVA/Ac–PVP blend film shows the peaks due to fluorescence X-rays, which are attributed to C, N and O atoms present in the host polymer matrix. For the $TiO_2$ NP-filled composite films, the fluorescence X-rays of Ti due to $K_{\alpha 1}$, $K_{\beta 1}$, $L_{\alpha 1}$ X-rays (characteristic or fluorescent X-rays) are observed at energies 4.5, 4.9 and 0.45 keV, respectively. It can be seen that there is an increase in intensity of the characteristic X-ray peaks due to Ti with an increase in the concentration of $TiO_2$ NPs.

### 3.2 *Optical analysis*

*3.2a Study of energy bandgap*: Quantitative analysis of optical properties of polymer nanocomposites is of great

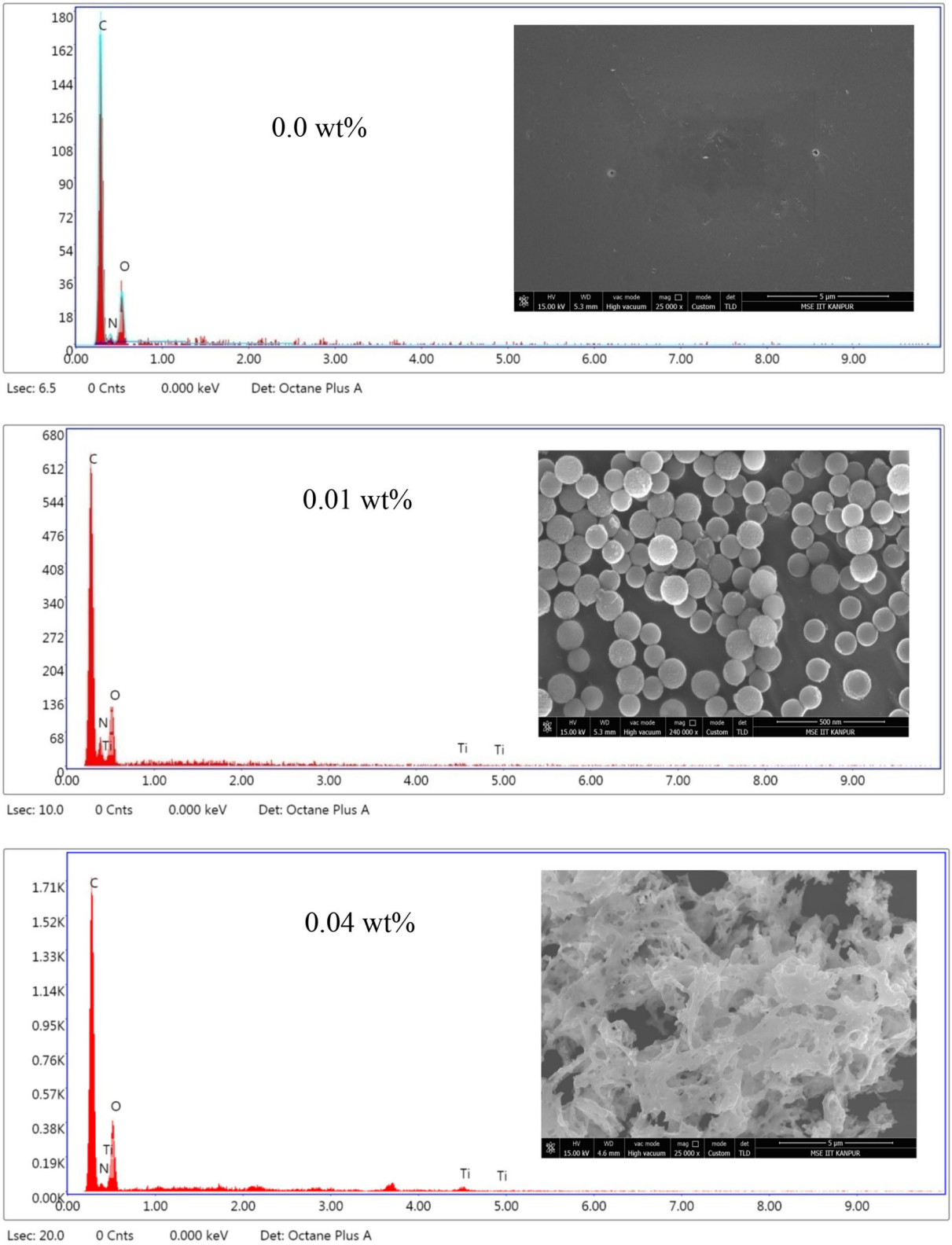


**Figure 1.** EDS spectra (plots of registered events or Counts versus the energy of emitted characteristic X-rays) for pure and $TiO_2$ NPs-filled PVA/Ac–PVP blend composites (inset: the SEM images).

importance in order to determine the electronic density of states and changes in the optical band structure of the material as a result of adding filler. In order to study the optical properties of PVA/Ac–PVP blend system, the spectral distribution of absorbance was obtained as the primary data, as a function of wavelength, in the range

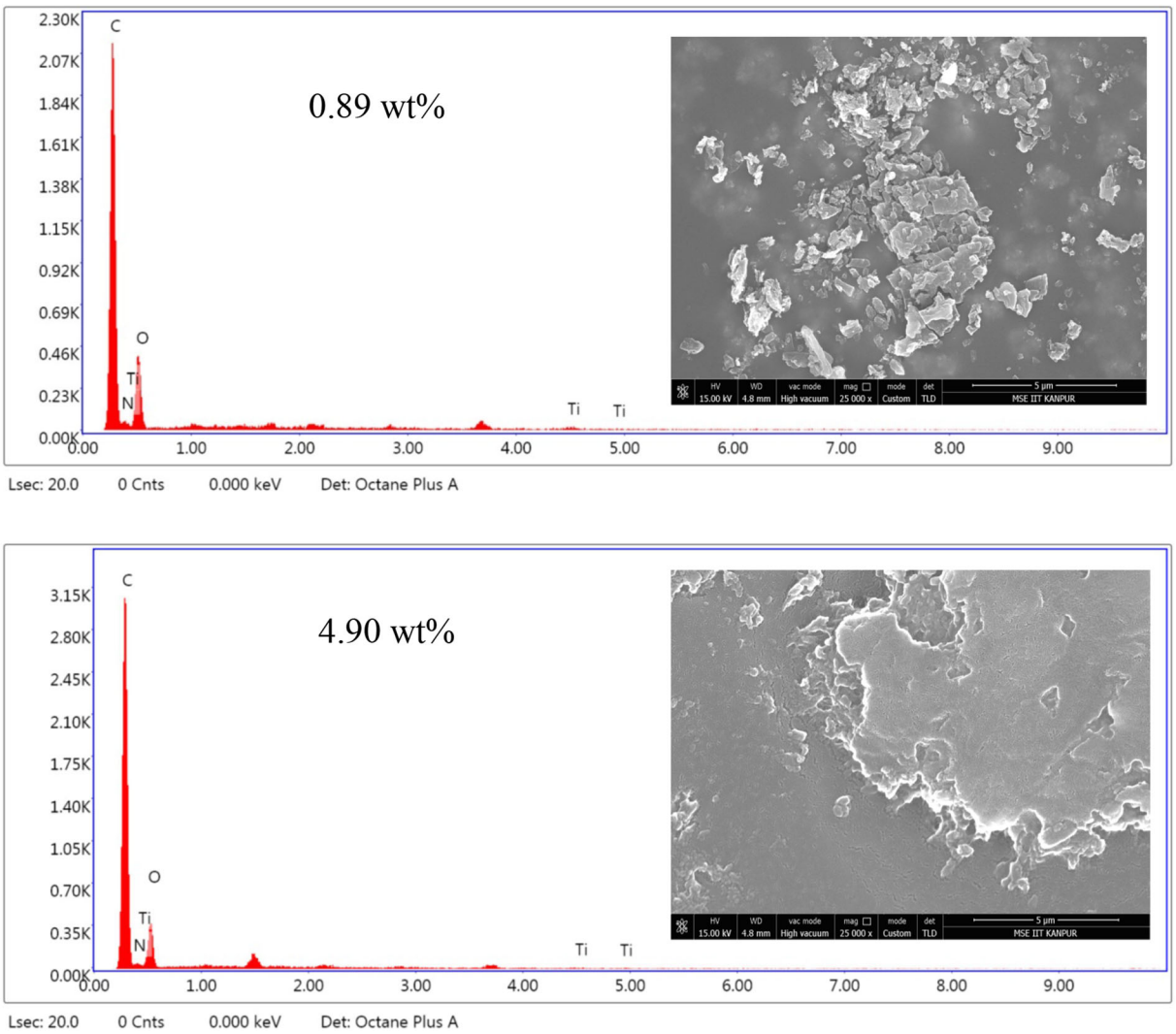


**Figure 1.** continued

**Table 1.** EDS peak assignments of pure and $TiO_2$ NPs-filled PVA/Ac–PVP blend composites.

| Element | Assignment | Energy (k eV) |
|---|---|---|
| C | $K_{\alpha 1}$ | 0.277 |
| N | $K_{\alpha 1}$ | 0.392 |
| O | $K_{\alpha 1}$ | 0.525 |
| Ti | $K_{\alpha 1}$ | 4.5 |
| Ti | $K_{\beta 1}$ | 4.9 |
| Ti | $L_{\alpha 1}$ | 0.45 |

varying from 190 upto 1000 nm. This data was further exploited in order to determine the various optical parameters.

When a polymeric material is exposed to electromagnetic radiation, a part of the light gets absorbed, a part of it gets transmitted and the remaining part of it gets reflected. So, from the law of conservation of energy, it can be established that the following equation holds good.

$$A + T + R = 1 \tag{2}$$

where $A$ is the absorbance, $T$ is the transmittance and $R$ is the reflectance. The value of $T$ is determined from the absorbance data by using the following relation.

$$T = 10^{-A} \tag{3}$$

Using equations (2) and (3), the value of $R$ is determined. Figure 2a shows the spectral distribution of $A$ as a function of wavelength ($\lambda$). Figure 3a and b represents the variation of $T$ and $R$ as a function of wavelength ($\lambda$) of the incident UV/visible radiation. A major absorbance peak at 220 nm [52] and absorbance edge at 290 nm in the absorbance spectra of pure PVA/Ac–PVP blend are due to $n \rightarrow \pi^*$ and $\pi \rightarrow \pi^*$ transitions, attributed to C=C and C=O bonds, respectively [53].

The UV–visible spectra of $TiO_2$ show that the absorbance has increased with an increase in the FL of $TiO_2$ NPs in PVA/Ac - PVP blend, due to the presence of light absorbing centres in the form of CTCs, formed as a result of

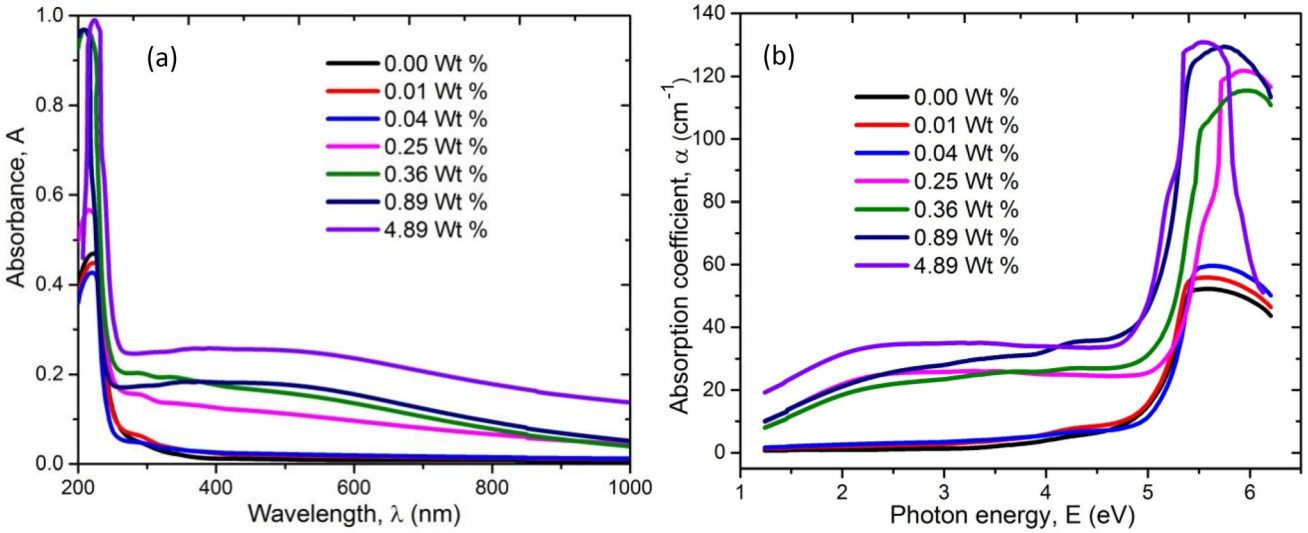


**Figure 2.** (**a**) The plot of absorbance (*A*) *vs.* wavelength ($\lambda$). (**b**) Plot of absorption coefficient ($\alpha$) *vs.* photon energy (*E*) for pure and $TiO_2$ NP-filled PVA/Ac–PVP blend composite.

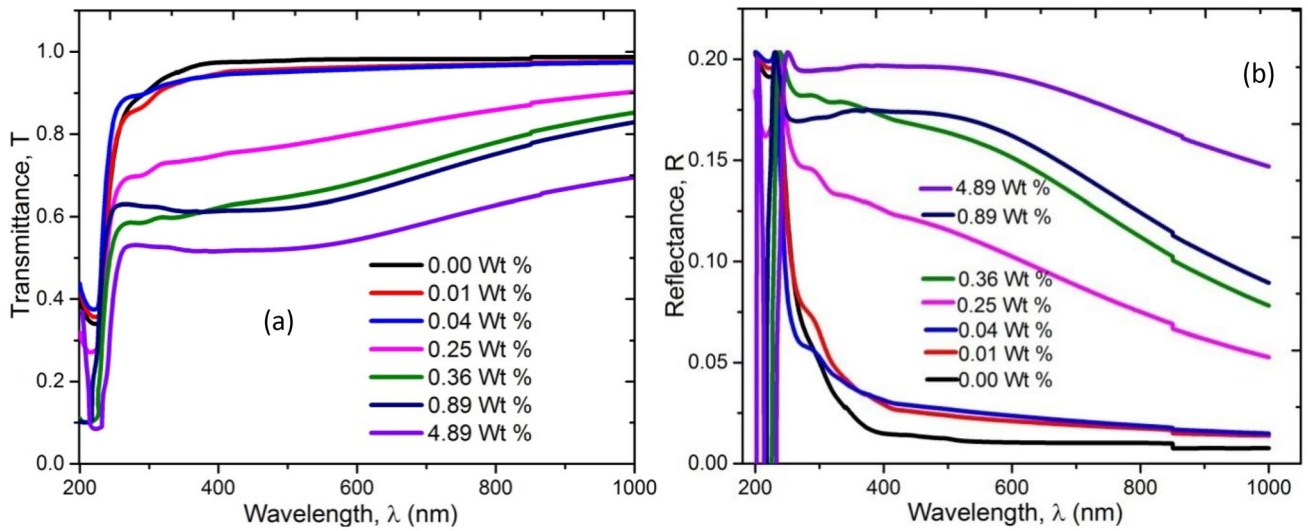


**Figure 3.** (**a**) The plot of transmittance (*T*) *vs.* wavelength ($\lambda$). (**b**) Plot of reflectance (*R*) *vs.* wavelength ($\lambda$) for pure and $TiO_2$ NP-filled PVA/Ac–PVP blend composite.

interaction of $TiO_2$ NPs with molecular sites in the PVA/Ac–PVP blend. Pure PVA/Ac–PVP blend sample shows very less or no absorbance in the visible region (that is, for wavelengths varying from 400 up to 800 nm). In the case of $TiO_2$ NP-filled PVA/Ac–PVP sample, an absorption band in the wavelength region ranging from 200 up to 400 nm is observed as a result of Ti–O band. Also, absorption bands at 360 and 450 nm are observed due to the electronic transitions which occur in the $TiO_2$ NPs and its aggregates in $TiO_2$-filled samples (especially in filled samples with FLs 0.89 and 4.89 wt%), on absorption of incident photons of suitable energies.

The attenuation of radiation (electromagnetic radiation in the UV and visible regions) by the sample can be more precisely studied by using the data of its absorption co-efficient ($\alpha$) as a function of photon energy (see figure 2b); the value of absorption coefficient being determined by equation (4).

The activation energy ($E_a$) for optical transition is estimated from the slope and *y*-intercept of the linear portion of a plot of absorption co-efficient ($\alpha$) as a function of photon energy (*E*). The values of $E_a$ are listed in table 2.

$$\alpha = 2.303 \times \frac{A}{d} \tag{4}$$

In equation (4), *A* is the absorbance and *d* is the thickness. Energy bandgap ($E_a$) may be attributed to the electronic transitions taking place from the highest occupied

**Table 2.** Values of activation energy ($E_a$) for optical transitions and optical bandgap ($E_{IAT}$ and $E_{DAT}$) due to indirect allowed transition (IAT) and direct allowed transition (DAT) transitions, respectively (all expressed in eV), for pure and $TiO_2$ NP-filled PVA/Ac–PVP blend composite.

| FL (wt%) | $E_a$ (eV) | | $E_{IAT}$ (eV) | | $E_{DAT}$ (eV) |
|---|---|---|---|---|---|
| | $E_{a1}$ | $E_{a2}$ | $E_{IAT1}$ | $E_{IAT2}$ | $E_{DAT1}$ |
| 0.00 | 5.12 ± 0.021 | 3.33 ± 0.002 | 4.90 ± 0.012 | 2.98 ± 0.002 | 5.28 ± 0.01 |
| 0.01 | 4.89 ± 0.012 | 3.22 ± 0.009 | 4.80 ± 0.017 | 2.64 ± 0.008 | 5.17 ± 0.062 |
| 0.04 | 5.13 ± 0.041 | — | 4.90 ± 0.057 | 2.04 ± 0.008 | 5.25 ± 0.052 |
| 0.25 | 5.03 ± 0.007 | 2.33 ± 0.039 | 4.84 ± 0.082 | 1.68 ± 0.032 | 5.21 ± 0.031 |
| 0.36 | 4.94 ± 0.012 | 3.43 ± 0.015 | 4.64 ± 0.010 | 1.65 ± 0.036 | 5.21 ± 0.089 |
| 0.89 | 4.80 ± 0.047 | — | 4.86 ± 0.041 | — | 5.33 ± 0.006 |
| 4.89 | 4.72 ± 0.003 | 1.24 ± 0.043 | 4.77 ± 0.042 | 2.82 ± 0.013 | 5.14 ± 0.006 |

molecular orbital to the lowest unoccupied molecular orbital of the host polymeric material, on absorption of incident light photons of suitable energy. Since $TiO_2$ NPs are efficient UV absorbers, $TiO_2$ NP-filled PVA/Ac–PVP composite films show notable changes in the ultra-violet optical spectra. Energy ($E$) of the incident photon (in eV) is calculated by using the following equation:

$$E = \frac{1.24 \times 10^{-6}}{\lambda}. \tag{5}$$

In equation (5), $\lambda$ is the wavelength of the incident photon (in metre).

Absorption coefficient ($\alpha$) and optical bandgap ($E_g$) for pure and $TiO_2$ NP-filled PVA/Ac–PVP blend composite samples obeys Tauc's expression. $E_g$ values are calculated using Mott–Davis equation [54,55], which follows:

$$\alpha = \frac{\beta(h\nu - E_g)^{\gamma}}{h\nu}. \tag{6a}$$

In equation (6a), $\beta$ is a constant, $E_g$ is the energy bandgap, $\gamma$ is an empirical index and $h\nu$ is the incident (absorbed) photon energy. The values of $\gamma$ varies as follows; it is $1/2$ for direct allowed transition (DAT), $3/2$ for direct forbidden transition (DFT), 2 for indirect allowed transition (IAT) and 3 for indirect forbidden transition (IFT), respectively.

A plot of $\alpha$ against $h\nu$ (figure 2b) is used to determine the value of $E_a$ for pure and $TiO_2$ NP-filled PVA/Ac–PVP blend composite samples, by extrapolating the linear region of the rising edge of the major absorption head to the energy axis (that is, to zero absorbance value). The values of $E_a$ for pure and $TiO_2$ NP-filled PVA/Ac - PVP blend samples are listed in table 2. It can be seen that, the major absorption edge of $TiO_2$-filled PVA/Ac–PVP polymer nanocomposite shows a red shift (with the major absorption edge moving towards higher $\lambda$-values) with an increase in FL. Thus, it should be noted that the energy bandgap value decreases as the FL increases, accompanied by the formation of intermediate absorption band due to the formation of CTCs, as a result of the interaction between $TiO_2$ NPs and the polymer molecules of the host matrix. The activation energy for pure PVA/Ac–PVP blend is 5.12 eV, and it has reduced to 4.72 eV for titania-filled composite films with FL 4.89 wt%. Optical absorption data were used to extract the bandgap values corresponding to all the four types of transitions, by extrapolating the $(\alpha h\nu)^{(1/2)}$ *vs.* $E$, $(\alpha h\nu)^{(2)}$ *vs.* $E$, $(\alpha h\nu)^{(2/3)}$ *vs.* $E$ and $(\alpha h\nu)^{(3)}$ *vs.* $E$ graphs to zero photon energy (see figures 4a, b and 5a, b). The values of these energies are tabulated in tables 2 and 3, with their respective error values, for the major absorption edge and their respective intermediate states. Although the plots of $(\alpha h\nu)^{(1/2)}$ *vs.* $h\nu$ show best fit, other transitions also show good fitting. Hence, all the four transitions are represented here. The decrease in the energy bandgap values of $TiO_2$-filled PVA/Ac–PVP blend is due to the optoelectronic properties of the $TiO_2$ NPs. The interaction of $TiO_2$ with the polymer molecules is such that $TiO_2$ interacts with PVA/Ac–PVP to form CTCs via inter and intramolecular hydrogen bonding. Literature reveals instances where the components of polymeric blend form CTC with the added filler [56,57]. A study on tin sulphide (SnS)-filled PVA/Ac–PVP blend reported that the use of 0.5 wt% filler-incorporated material can be used as an efficient UV blocker [11]. In the present study, it is seen that the incorporation of $TiO_2$ NPs has not only enhanced the absorption of electromagnetic radiation in the UV region, but has also drastically enhanced its absorbance in the visible region, where the pure PVA/Ac–PVP blend showed almost no absorbance. This property of this composite film can be exploited to use the composite as an efficient optoelectronic material, when a material with greater absorbance in UV and visible regions is required. They can also be used in packing materials, which are meant to protect its contents from UV and visible light.

The energy bandgap of the composite sample for optical transitions (electronic transitions taking place by the absorption of incident photon of suitable energy) is

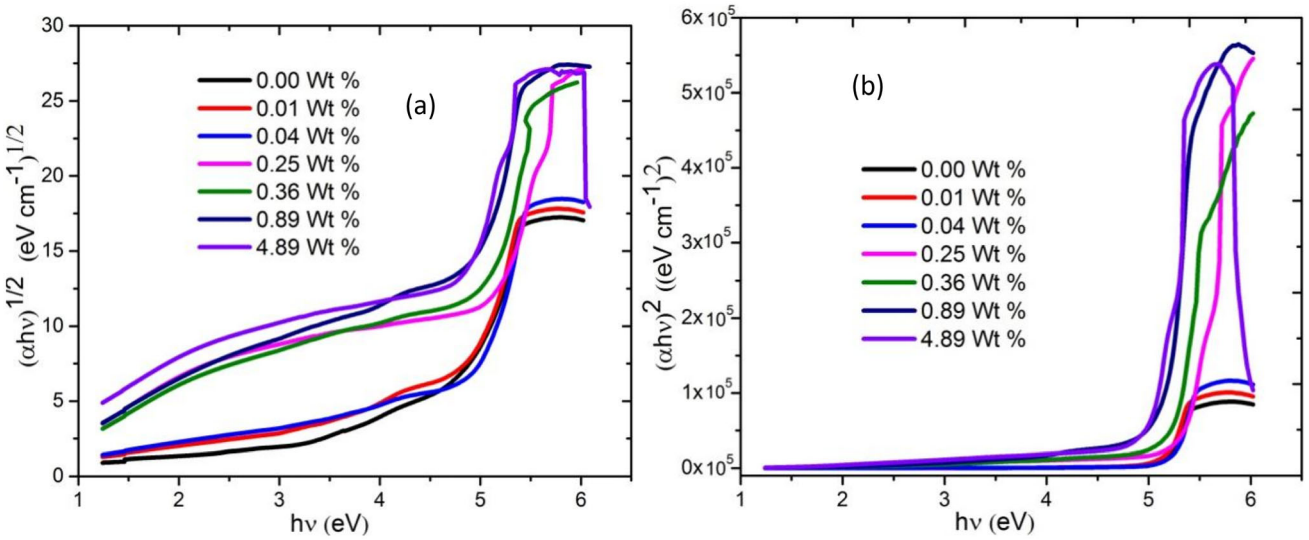


**Figure 4.** (**a**) The plots of $(\alpha h\nu)^{(1/2)}$ *vs.* photon energy ($E$). (**b**) Plots of $(\alpha h\nu)^2$ *vs.* photon energy ($E$) for pure and $TiO_2$ NP-filled PVA/Ac–PVP blend composite.

confirmed by plotting a graph of $h\nu\sqrt{\varepsilon_2}$ against $h\nu$, according to equation (6b) [58,59]:

$$h^2\nu^2\varepsilon_2 \approx \left(h\nu - E_{g1}\right)^2. \tag{6b}$$

In equation (6b), $h\nu$ is the incident photon energy and $\varepsilon_2$ is the imaginary part of dielectric constant.

The IAT values for $TiO_2$ NP-filled PVA/Ac–PVP blend composites were confirmed by plotting a graph of $h\nu\sqrt{\varepsilon_2}$ against $h\nu$ (refer equation (6b)). Figure 5c shows the plot of $h\nu\ (\varepsilon_2)^{(1/2)}$ *vs.* $h\nu$, for various FLs. The values of bandgap obtained from this graph are represented as $E\ \varepsilon_i$ in table 3.

*3.2b Study of dispersion parameters*: Refractive index ($n$) is a characteristic property of the material, which determines the speed of light in that medium. Complex refractive index (RI) of the material is denoted as '$N$' and is used to determine the various optical features of the material, the modification of which is helpful for tailoring this material, for its use in specific optoelectronic devices. Complex RI is given by equation (7):

$$N = n - iK. \tag{7}$$

In equation (7), the real part '$n$' is the normal RI, which accounts for the dispersion properties in the material, while the imaginary part '$K$' is the extinction coefficient, which represents the rate of dissipation of incident electromagnetic wave in the dielectric medium (in this case the dielectric medium is the polymeric matrix). The value of '$K$' is determined using the following relation:

$$K = \frac{\alpha\lambda}{4\pi}. \tag{8}$$

Refractive index '$n$' is determined by using the Fresnel formula [60], and it is given by equation (9):

$$n = \left(\frac{1+R}{1-R}\right) - \sqrt{\frac{4R}{(1-R)^2} - k^2} \tag{9}$$

Figure 6 represents the graph of $n$ with respect to $\lambda$. It can be seen that the nature of graph shows two different features. In the visible region, the values of $n$ decreases with increase in wavelength, and reaches a constant value at higher wavelength, but in the UV region, it is seen that there are a number of peaks, which are attributed to the absorbing centres or CTCs that are introduced in the polymer structure as a result of incorporating the $TiO_2$ NPs. It is also to be noted that, the value of '$n$' increases on adding $TiO_2$. This change in the value of '$n$' is due to the structural changes induced by the titania NPs in PVA/Ac–PVP blend, as confirmed from the FT-IR analysis [42]. There are CTCs formed in the composite as a result of hydrogen bonding between the polymer and $TiO_2$ NPs. The CTC acts as absorbing centres and their distribution in the nanocomposite films results in an enhancement in the value of '$n$'. The materials with high RI may be used in the fabrication of optoelectronic devices. Thus, $TiO_2$-filled PVA/Ac–PVP nanocomposite can be used as a suitable candidate for the fabrication of optoelectronic devices.

*3.2c Optical conductivity*: Optical conductivity ($\sigma$) is an important optical parameter, which reveals the optoelectronic characteristics of a material. Optical conductivity of the composite material is determined as a function of $\alpha$ [61] and $n$, and its nature (variation of $\sigma$ *vs.* photon energy (see figure 7a)) resembles the nature of $\alpha$. This parameter is found to increase with FL in case of titania NP-filled PVA/Ac–PVP blend due to an increase in number density of charge carriers and due to the formation of CTCs as a result of incorporating the $TiO_2$ NPs in PVA/Ac–PVP blend. When electromagnetic radiation of suitable frequency is

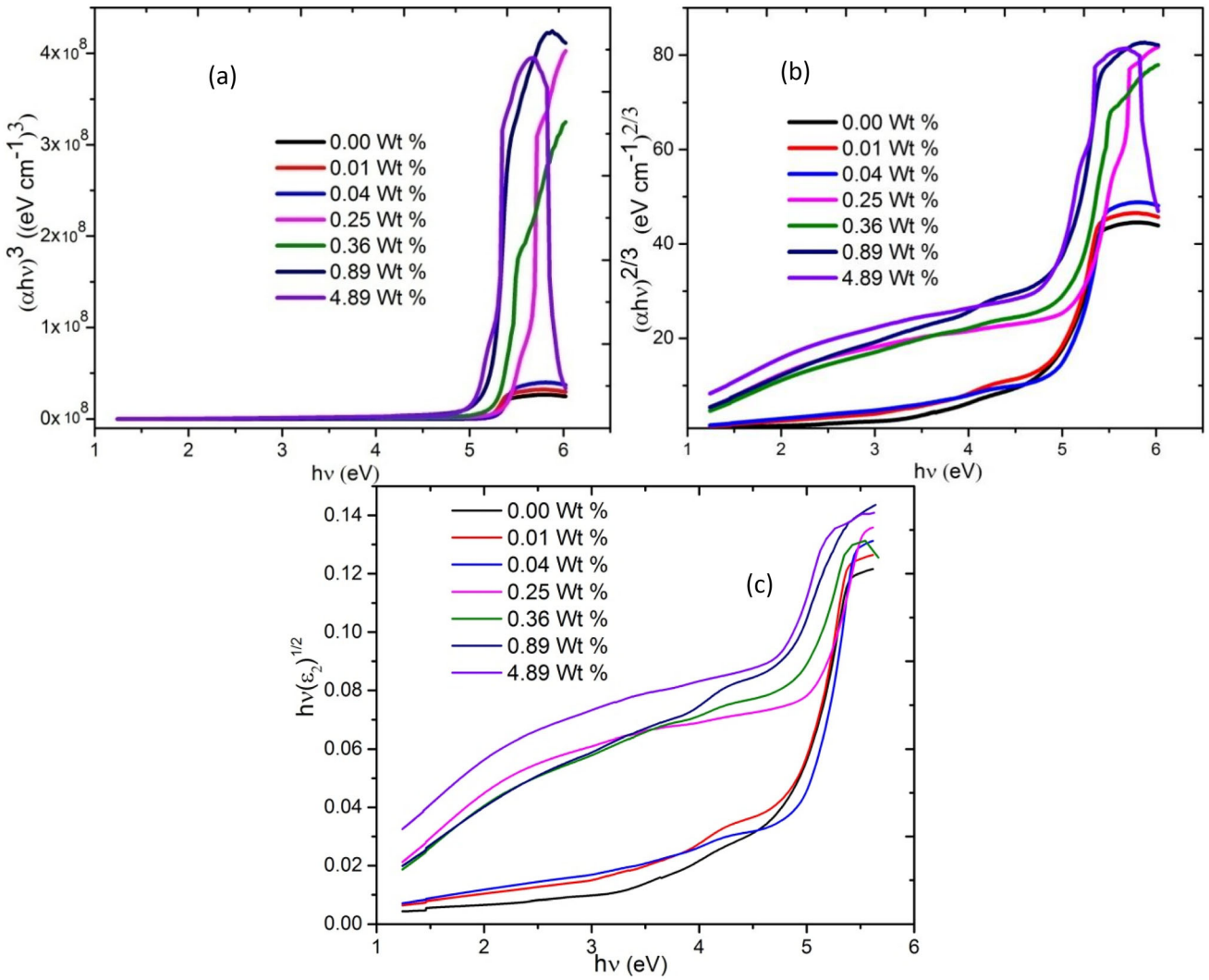


**Figure 5.** (**a**) The plots of $(\alpha h\nu)^3$ *vs.* photon energy ($E$). (**b**) Plots of $(\alpha h\nu)^{2/3}$ *vs.* photon energy ($E$) for pure and $TiO_2$ NP-filled PVA/Ac–PVP blend composite. (**c**) Plot of $h\nu(\varepsilon_2)^{1/2}$ *vs.* $h\nu$

**Table 3.** Values of optical bandgap ($E_{IFT}$ and $E_{DFT}$) due to indirect forbidden transition (IFT) and direct forbidden transition (DFT) transitions, respectively (all expressed in eV), for pure and $TiO_2$ NP-filled PVA/Ac–PVP blend composite.

| FL (wt%) | $E_{IFT}$ (eV) | $E_{DFT}$ (eV) | | $E_{\varepsilon i}$ (eV) | |
|---|---|---|---|---|---|
| | $E_{IFT1}$ | $E_{DFT1}$ | $E_{DFT2}$ | $E\varepsilon_{i1}$ | $E\varepsilon_{i2}$ |
| 0.00 | 5.32 ± 0.012 | 5.10 ± 0.024 | 3.1 ± 0.006 | 4.87 ± 0.010 | 2.95 ± 0.014 |
| 0.01 | 5.20 ± 0.058 | 4.91 ± 0.00 6 | — | 4.76 ± 0.030 | 2.75 ± 0.020 |
| 0.04 | 5.31 ± 0.040 | 5.04 ± 0.005 | 2.51 ±0.013 | 4.79 ± 0.020 | 2.28 ± 0.010 |
| 0.25 | 5.32 ± 0.001 | 5.32 ± 0.074 | 2.13 ± 0.004 | 4.70 ± 0.012 | 1.72 ± 0.015 |
| 0.36 | 5.26 ± 0.067 | 5.08 ± 0.067 | — | 4.62 ± 0.040 | 1.71 ± 0.021 |
| 0.89 | 5.24 ± 0.005 | 5.02 ± 0.009 | — | 4.68 ± 0.032 | — |
| 4.89 | 5.20 ± 0.038 | 4.89 ± 0.004 | 1.63 ± 0.007 | 4.56 ± 0.019 | — |

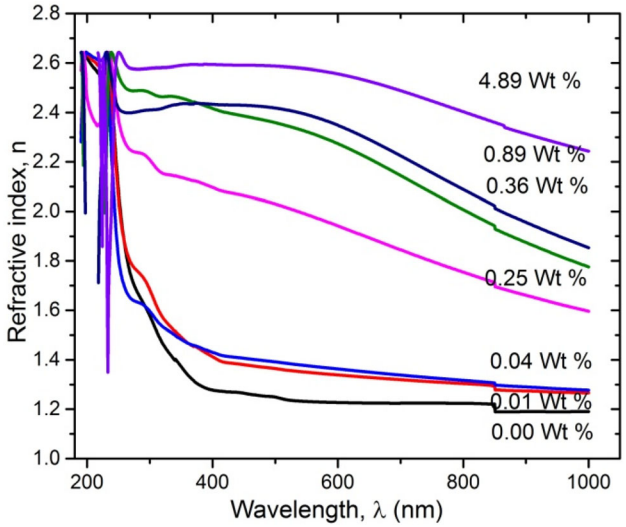


**Figure 6.** Variation of refractive index ($n$) *vs.* wavelength ($\lambda$) for pure and $TiO_2$ NP-filled PVA/Ac–PVP blend composite.

incident on the $TiO_2$ NP-filled polymeric composite, there is an excitation of charge carriers across and within the bandgap, resulting in an enhancement of its optical conductivity.

$$\sigma = \frac{\alpha nc}{4\pi} \tag{10}$$

It can be observed that the value of $\sigma$ tends to remain constant in the low photon energy region, signifying that the energy of the incident radiation in this region is not sufficient for excitation of electrons (in the material) across the bandgap, whereas the value of $\sigma$ increases at higher energy (of incident photons) implying that more number of charge carriers are excited once the incident photon energy crosses a certain threshold. Increase in the optical conductivity of the composite material with an increase in the concentration of $TiO_2$ NPs may be attributed to the increase in carrier concentration due to the formation of CTCs as well as the introduction of impurity states in the optical bandgap of the polymeric material as a result of incorporating $TiO_2$ NPs as the filler.

Penetration depth is a measure of how deep the incident photons (quanta of electromagnetic radiation) can penetrate into the material, and it is denoted by the symbol $\delta_p$ (or $\delta$). The value of $\delta$ is determined using equation (11).

The variation of $\delta$ (expressed in cm) *vs.* incident photon energy ($E = h\nu$) for pure and $TiO_2$ NP-filled PVA/Ac–PVP blend composite is shown in figure 7b. It is noted that there is a significant decrease in $\delta$ with an increase in photon energy, especially in the composite films. As expected, there is a marked decrease in $\delta$ beyond the photon energy corresponding to the absorption edge.

$$\delta p = \frac{1}{\alpha} \tag{11}$$

Complex dielectric function or permittivity is a complex quantity and is represented as follows:

$$\varepsilon^* = \varepsilon_1 - i\varepsilon_2. \tag{12}$$

The real and imaginary parts of dielectric function can be related to $n$ and $k$, and are represented by equations (13) and (14).

$$\varepsilon_1 = n^2 - K^2 \tag{13}$$

$$\varepsilon_2 = 2nK \tag{14}$$

The real part of dielectric constant ($\varepsilon_1$) represents the energy density of states which are responsible for the scattering of light radiation (which is incident on the samples) due to the polarization of the dipoles in the samples

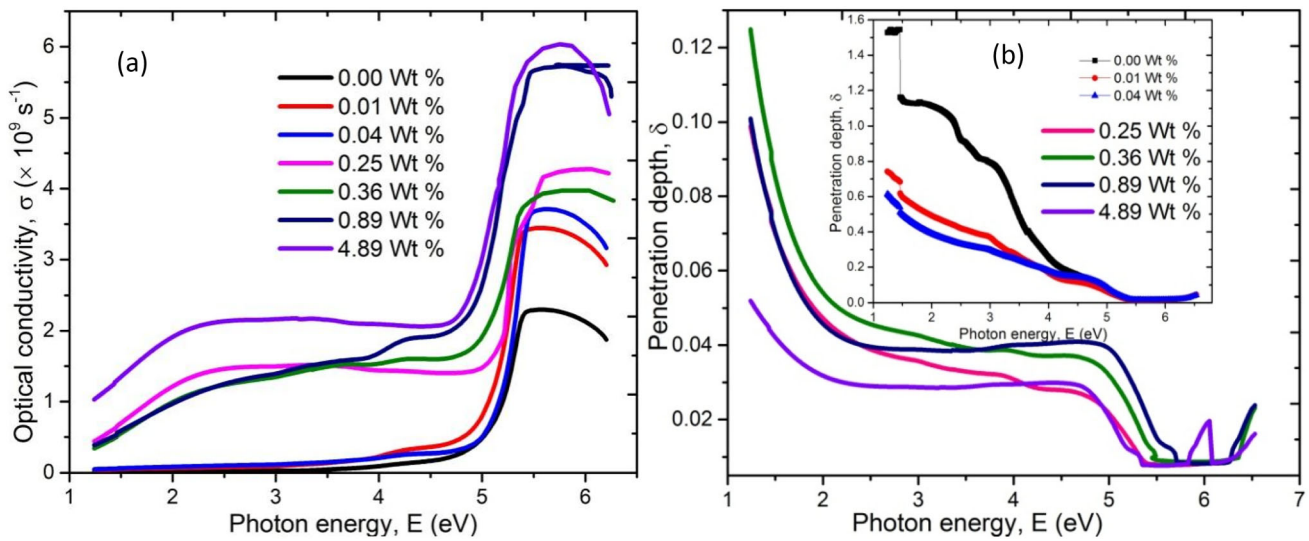


**Figure 7.** (**a**) Plot of optical conductivity ($\sigma$) *vs.* photon energy ($E$). (**b**) Plot of penetration depth ($\delta$, expressed in cm) *vs.* photon energy ($E$) for pure and $TiO_2$ NP-filled PVA/Ac–PVP blend composite.

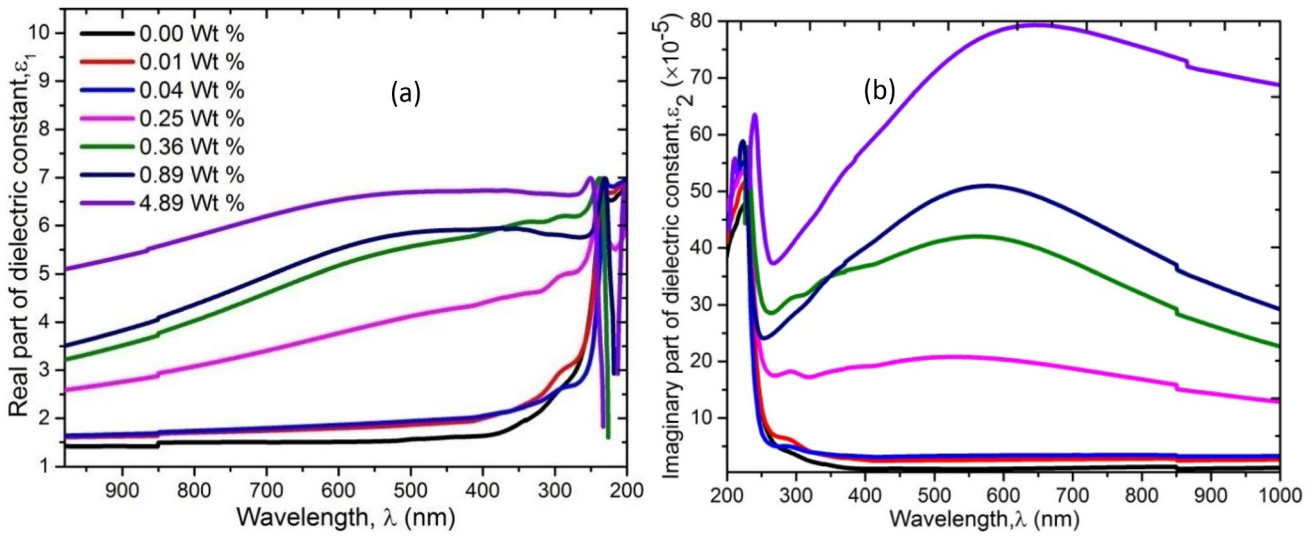


**Figure 8.** (**a**) Variation of $\varepsilon_1$ *vs.* wavelength ($\lambda$). (**b**) Plot of $\varepsilon_2$ *vs.* wavelength ($\lambda$) for pure and $TiO_2$ NP-filled PVA/Ac–PVP blend composite.

because of the incident electromagnetic radiation. Further, this quantity affects the speed of light. The imaginary part of dielectric constant ($\varepsilon_2$) accounts for energy absorbed due to dipole motion [62]. Figure 8a and b represents the real and imaginary dielectric constants as a function of $\lambda$, for pure and $TiO_2$ NP-filled PVA/Ac–PVP blend composite.

It can be seen from figure 8a that $\varepsilon_1$ has greater value when compared to $\varepsilon_2$. From this figure, it can be noticed that the values of $\varepsilon_1$ increases with an increase in FL of $TiO_2$ in PVA/Ac–PVP blend, at all wavelengths. This increase may be attributed to the increase in the polarization of the dipoles due to increase in density of states resulting from the incorporated $TiO_2$ NP, which forms CTC with the functional groups present in the side chains of the polymer. The increase in value of imaginary part of dielectric constant with the FL suggests the interactions taking place between the NPs and the PVA/Ac–PVP blend polymer matrix, which improves the amorphousness of the filler-incorporated samples.

*3.2d Dissipation factor (tan δ)*: Dissipation factor (tan $\delta$) is the ratio of the loss of energy to the storage of energy. In other words, it is the ratio of the imaginary part of dielectric constant to the real part of dielectric constant. This quantity measures the rate of loss of power of a mechanical oscillator. In fact, tan $\delta$ is an effective parameter to decide the usefulness of the nanocomposite material under study; that is, it determines its suitability to be a good dielectric material for use in electrical and optical applications. Dissipation factor (tan$\delta$) is determined using equation (15) [63].

$$\tan\delta = \frac{\varepsilon_2}{\varepsilon_1} \tag{15}$$

Figure 9 represents the graph of tan $\delta$ against frequency for pure and $TiO_2$ NP-incorporated polymer blend films. It can be seen that tan $\delta$ exhibits a very low value of the order of $10^{-5}$. An enhancement in the tan $\delta$ is observed with the incorporation of $TiO_2$ NPs, which is due to the formation of new defect states in the energy bandgap of polymer that act as dipole levels, resulting in the enhancement of dielectric behaviour.

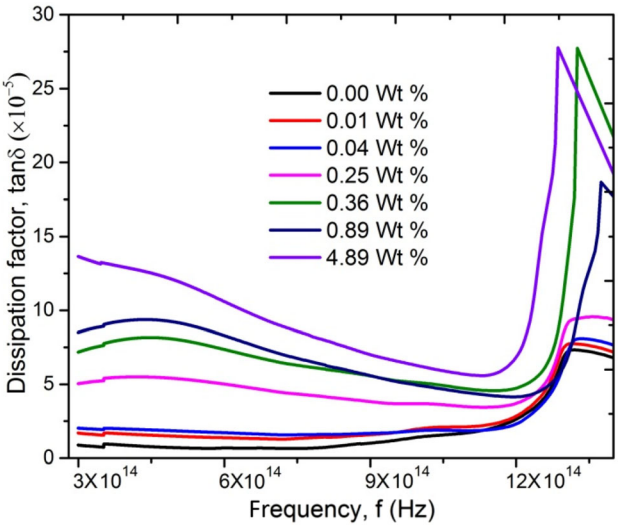


**Figure 9.** Plot of dissipation factor (tan $\delta$) against frequency for pure and $TiO_2$ NP-filled PVA/Ac–PVP blend composite.

*3.2e Volume and surface energy loss functions*: Volume energy loss function (VELF) and surface energy loss functions (SELF) are the parameters that reflect the amount of energy absorbed by the bulk and surface of the material, respectively, due to single-electron transitions [64]. VELF and SELF can be determined as a function of real and imaginary parts of dielectric constant, which are represented in the following equations [61,62].

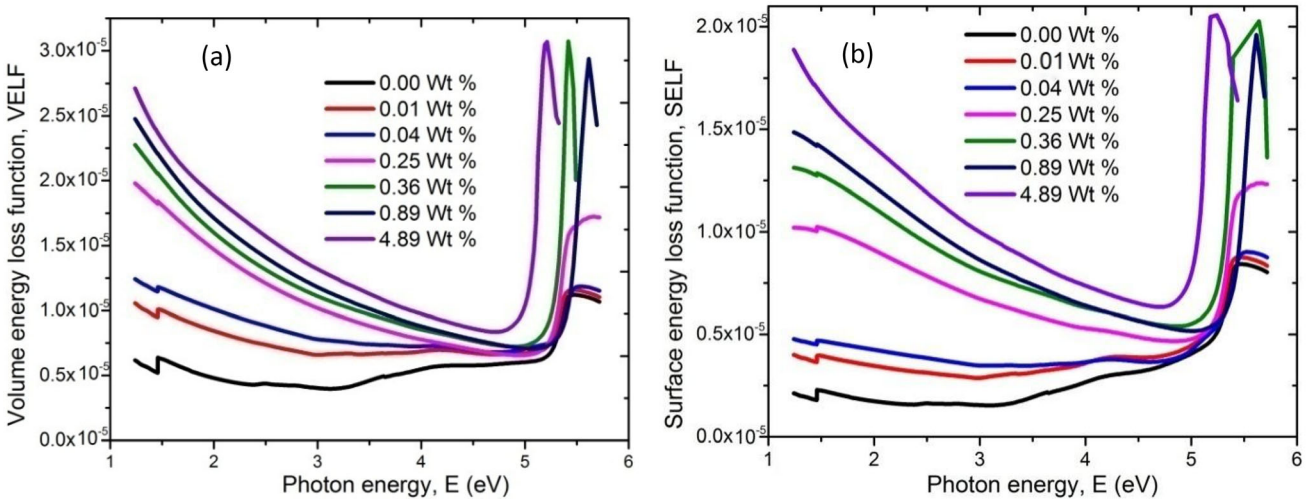


**Figure 10.** (**a**) Variation of volume energy loss function *vs.* photon energy ($E$). (**b**) Variation of surface energy loss function *vs.* photon energy ($E$) for pure and $TiO_2$ NP-filled PVA/Ac–PVP blend composite

$$\text{VELF} = \frac{\varepsilon_2}{\varepsilon_1^2 + \varepsilon_2^2} \tag{16}$$

$$\text{SELF} = \frac{\varepsilon_2}{(\varepsilon_1 + 1)^2 + \varepsilon_2^2} \tag{17}$$

Figure 10a and b represents the nature of VELF and SELF as a function of photon energy ($h\nu$) for pure and $TiO_2$ NP-filled PVA/Ac–PVP blend. It can be seen from the figure 10a and b that the value of both these functions increase with the increase in FL, and also that VELFs are having higher values compared to SELFs.

*3.2f Study of dispersion energy parameters*: The study of dispersion behaviour in polymer-filled samples is of great importance, as it reveals the usefulness of the sample for fabricating optoelectronic devices such as for those used in optical communications. Wemple and Didomenico model [65–67] is used to study the disorder in the system. This model employs single oscillator concept to determine the optical energy parameters by assuming each atom in the sample to be an oscillator. According to this model, the dependence of $n$ on the photon energy in the region less than $E_g$ is given by the equation (18):

$$n^2 - 1 = \frac{E_o E_d}{E_o^2 - (h\nu)^2} \tag{18}$$

In equation (18), $h\nu$ is the incident photon energy, $E_o$ is the single oscillator energy and $E_d$ is the dispersion energy, which resembles the disorder and gives the strength of interband optical transition.

RI ($n$) of the material exhibits lower value at lower wavelength, which may be attributed to the lattice vibration absorption. Thus, the lower energy region (which is linear region) of $(n^2-1)^{-1}$ against $(h\nu)^2$ (see figure 11) plot is linear fitted to obtain the slope and intercept, which are

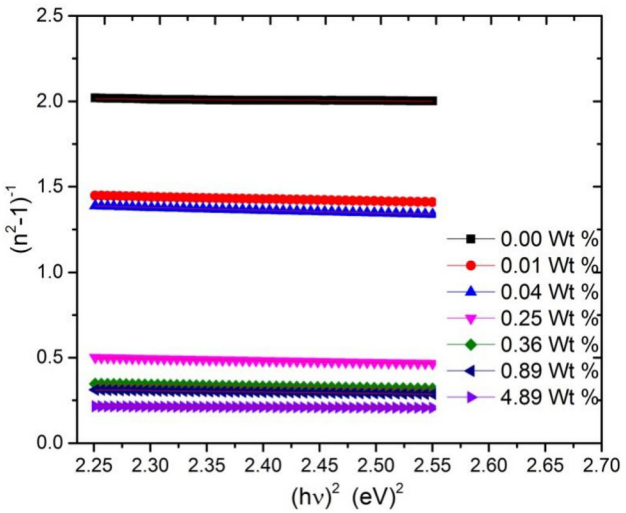


**Figure 11.** Plot of $(n^2-1)^{-1}$ *vs.* $(h\nu)^2$ for pure and $TiO_2$ NP-filled PVA/Ac–PVP blend composite (inset: SEM images).

further used to calculate $E_o$ and $E_d$. The values of $E_o$ and $E_d$ are tabulated in table 4.

The value of $E_o$ represents the average energy bandgap. From table 4, it can be seen that the value of $E_o$ is almost constant, on varying the FL of the composite from 0.01 upto 0.89 wt% with slight variation, and this value has increased to a value of 3.04 for the composite material with FL 4.89 wt%. But all these values are less than the value of this parameter in the case of pure PVA/Ac–PVP blend. This result reveals that the bandgap has decreased on incorporating $TiO_2$ NP compared to pure sample. This is due to the increased formation of localized sites in the energy bandgap of PVA/Ac–PVP blend. An increase in the $E_o$ value for the composite sample with FL 4.89 wt% compared to samples with lower FLs, may be attributed to the formation of crystalline regions in the sample of FL 4.89 wt% due to

**Table 4.** Values of $E_d$, $E_o$, $f$, $n_o$, $M_{-1}$, and $M_{-3}$ for pure and $TiO_2$ NP-filled PVA/Ac–PVP blend composite.

| FL (wt%) | $E_d$ (eV) | $E_o$(eV) | $f$ (eV)$^2$ | $n_o$ | $M_{-1}$ | $M_{-3}$ ((eV$^{-2}$)) |
|---|---|---|---|---|---|---|
| 0.0 | 1.99 | 4.51 | 8.97 | 1.20 | 0.44 | 0.016 |
| 0.01 | 1.86 | 3.27 | 6.08 | 1.25 | 0.56 | 0.053 |
| 0.04 | 3.35 | 2.54 | 8.50 | 1.52 | 1.32 | 0.204 |
| 0.25 | 3.70 | 2.14 | 7.91 | 1.65 | 0.57 | 0.042 |
| 0.36 | 4.24 | 2.37 | 10.04 | 1.67 | 1.78 | 0.318 |
| 0.89 | 4.94 | 2.45 | 12.10 | 1.73 | 2.01 | 0.335 |
| 4.89 | 10.76 | 3.04 | 32.71 | 2.13 | 3.54 | 0.382 |

aggregation of $TiO_2$ NPs, which results in the decrease of bandgap. The values of $E_d$ exhibit a gradual increase with an increase in FL, due to the variation in the structural order of the material. Since $E_d$ values represents strength of the interband transition, an increase in these values are attributed to increased transitions taking place from valence band to conduction band as a result of interaction of filler with the polymer. Similar results are observed in other polymer composites [68,69].

Oscillator strength ($f$) is determined by using the following equation [70].

$$f = E_d E_o \tag{19}$$

The values of oscillator strength for pure and $TiO_2$ NP-filled polymer blend are represented in table 4. It can be seen that the values of $f$ has decreased for composite films with FL up to 0.25 wt%, while it has increased for composite samples with FLs varying from 0.36 upto 4.89 wt%. Static refractive index ($n_o$) is one of the important parameters and is determined by considering the WDD dispersion equations at the photon energy equal to zero.

$$n_o = \sqrt{\frac{E_d}{E_o} + 1} \tag{20}$$

Table 4 lists the variation of $n_o$ for pure and $TiO_2$ NP-filled polymer blend composite films. The values of $n_o$ are found to increase with an increase in filler concentration.

The values of first-order spectral momenta ($M_{-1}$ and $M_{-3}$) for pure and $TiO_2$-filled polymer composite films are determined from single-oscillator constants, using the following pair of equations [71].

$$E_o^2 = \frac{M_{-1}}{M_{-3}}; \quad E_d^2 = \frac{M_{-1}^3}{M_{-3}} \tag{21}$$

The values of $M_{-1}$ and $M_{-3}$ are tabulated in table 4. These variations in the values of spectral momenta are due to the formation of co-ordination complexes, as a result of interaction between the polymer matrix and dopant ions. These quantities are associated with effective valence electrons.

*3.2g Determination of high frequency dielectric constant*: High frequency dielectric constant $\varepsilon_\infty$ was determined by two ways, using the refractive index data of $TiO_2$-filled PVA/Ac–PVP blends. Both of them are employed to get a reliable value for the dielectric constant for pure and the nanoparticle-incorporated samples.

The first method takes into account the free carrier and the lattice vibration modes of dispersion. In this method, the following equation (22) is used to determine high frequency dielectric constant [72].

$$\varepsilon = \varepsilon_{\infty 1} - \left(\frac{e}{4\pi c^2 \varepsilon_o}\right)\left(\frac{N}{m^*}\right)\lambda^2 \tag{22}$$

$$\varepsilon = n^2 \tag{23}$$

In equation (22), '$c$' is the velocity of light, $\varepsilon_o$ is permittivity of free space, having a value $8.854 \times 10^{-12}$ F m$^{-1}$, $N$ and $m^*$ are the free charge carrier concentration and effective mass of charge carriers, respectively. According to equations (22) and (23), a plot of $n^2$ against $\lambda^2$ (see figure 12) is used to determine the values of high frequency dielectric constant for pure and $TiO_2$-filled samples. It can

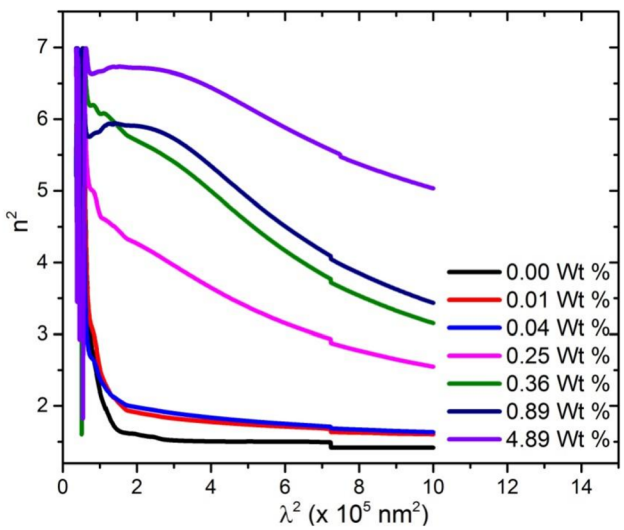


**Figure 12.** Plot of $n^2$ *vs* $\lambda^2$ for pure and $TiO_2$ NP-filled PVA/Ac–PVP blend composite.

**Table 5.** Values of dispersion parameters for pure and $TiO_2$ NP-filled PVA/Ac–PVP blend composite.

| FL (wt%) | $\varepsilon_\infty$ | $\omega_p^2$ ($\times 10^5$ $s^{-1}$) | $N/m^*$ ($\times 10^{37}$ $kg^{-1}$ $m^{-3}$) | $\varepsilon_{\infty 1}$ | $\lambda_o$ (nm) | $S_o(m^{-3})$ |
|---|---|---|---|---|---|---|
| 0.0 | 1.64 | 6.75 | 15.7 | 1.32 | 330.20 | 0.29 |
| 0.01 | 1.67 | 3.67 | 4.67 | 1.60 | 307.92 | 4.87 |
| 0.04 | 1.78 | 5.31 | 9.74 | 1.63 | 340.48 | 5.20 |
| 0.25 | 3.55 | 13.46 | 62.8 | 3.48 | 431.81 | 7.94 |
| 0.36 | 4.89 | 17.69 | 108.4 | 4.05 | 452.25 | 10.02 |
| 0.89 | 5.35 | 18.55 | 119.2 | 5.15 | 443.61 | 11.94 |
| 4.89 | 6.61 | 16.82 | 121.71 | 6.27 | 351.71 | 31.28 |

be seen that, for longer wavelengths, the dependence of $\varepsilon = n^2$ on $\lambda^2$ is found to be linear. Extrapolating the linear part to zero wavelengths gives the value of $\varepsilon_{\infty 1}$. Values of $N/m^*$ are calculated using the slope of this linear fit. These values are listed in table 5. When electron damping factor is very small compared to $\omega$, refractive index ($n$) can be expressed as shown in equation 24 [73].

$$n^2 = \varepsilon_\infty - \left(\frac{\omega_p^2}{\omega^2}\right) \tag{24}$$

In equation (24), $\omega$ is angular frequency of light and $\omega_p$ is plasma frequency. The value of $\omega_p$ is calculated by using equation (25),

$$\omega_p^2 = \frac{e^2 N}{\varepsilon_o m^*} \tag{25}$$

Table 5 lists the calculated values of $N/m^*$, $\omega_p$ and $\varepsilon_{\infty 1}$.

UV–visible spectra in the non-absorbing region or in the region of infinite wavelength are analysed to determine the optical parameters such as average inter-band oscillator wavelength ($\lambda_o$), infinite dielectric constant or high frequency dielectric constant ($\varepsilon_\infty = n^2$) and average oscillator strength ($S_o$) using the Moss model, according to which, the contribution of free carrier to dispersion is relatively small [74]. Hence, the data below the absorption edge are considered for analysis. The high frequency dielectric constant ($\varepsilon_{\infty 2}$) is determined using the following equation [75]. This method takes into account the contribution of bound carriers to dispersion.

$$\frac{1}{(n^2-1)} = \frac{\lambda_o^2}{(n_o^2-1)}\lambda^{-2} + (n_o^2-1)^{-1} \tag{26}$$

and

$$\frac{(n_o^2-1)}{\lambda_o^2} = S_o \tag{27}$$

According to equation (26), the values of $S_o$ and $\lambda_o$ are determined using the slope and intercept of $(n^2-1)^{-1}$ *vs.* $\lambda^{-2}$ graph. Figure 13 shows the plot of $(n^2-1)^{-1}$ *vs.* $\lambda^{-2}$, for different FLs of $TiO_2$-filled PVA/Ac–PVP blend. The value of $(n_o^2-1)^{-1}$ is determined by intersecting the linear region of this graph to $(n^2-1)^{-1}$ axis. Thus, the value of $n_o^2$ at $\lambda_o$ is determined. The value of $n_o^2$ denotes high frequency dielectric constant ($\varepsilon_{\infty 2}$). Although the values of high frequency dielectric constant $\varepsilon_{\infty 1}$ and $\varepsilon_{\infty 2}$ agree with each other, lattice vibrations and bound carriers in an empty lattice (in the transparent region) results in a small difference in their values.

*3.2h Nonlinear optical properties*: Nonlinear optical properties of the material are of great importance to decide their use in applications such as photo-electronic devices. Polymeric materials with low nonlinear refractive index ($n_2$) and nonlinear optical susceptibility ($\chi^{(3)}$) values are preferred as nonlinear media for optoelectronic applications [76,77]. Thus, the determination and study of nonlinear optical parameters are of great importance. The values of $E_o$, $E_d$ and $n_o$ are used to calculate the nonlinear optical parameters.

Linear optical susceptibility $\chi^{(1)}$ signifies the stimuli of the polymeric material to the incident radiation and is determined using the following equation.

$$\chi^{(1)} = \frac{E_d}{4\pi E_o} \tag{28}$$

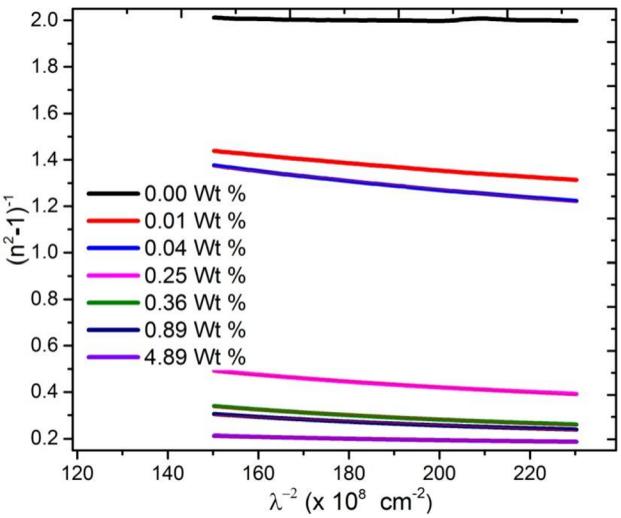


**Figure 13.** Plot of $(n^2-1)^{-1}$ *vs.* $\lambda^{-2}$ for pure and $TiO_2$ NP-filled PVA/Ac–PVP blend composite.

**Table 6.** Values of nonlinear optical parameters for pure and $TiO_2$ NP-filled PVA/Ac–PVP blend composite.

| FL (wt%) | $\chi^{(1)}$ | $\chi^{(3)}(\times 10^{-16}$ esu) | $n_2(\times 10^{-17}$esu) |
|---|---|---|---|
| 0.0 | 0.035 | 2.55 | 1.3 |
| 0.01 | 0.045 | 6.97 | 3.5 |
| 0.04 | 0.105 | 206.6 | 85.4 |
| 0.25 | 0.137 | 598.8 | 228.1 |
| 0.36 | 0.284 | 11059.1 | 4161.4 |
| 0.89 | 0.321 | 18049.6 | 6556.2 |
| 4.89 | 0.563 | 170797.8 | 50389.1 |

Table 6 shows the tabulated values of $\chi^{(1)}$. It infers that the values of $\chi^{(1)}$ has increased with the increase in the FL, which may be attributed to the increase in the response of the material in the form of increase in the number of transitions taking place from highest occupied molecular orbital to lowest unoccupied molecular orbital by absorbing the incident photons, due to incorporation of $TiO_2$ NPs.

Third-order nonlinear susceptibility, $\chi^{(3)}$, can be determined using the following equation.

$$\chi^{(3)} = A\left(\frac{E_d}{4\pi E_o}\right)^4 \tag{29}$$

Equation (22) can also be written as,

$$\chi^{(3)} = A{\chi^{(1)}}^4 \tag{30}$$

where, $A$ is a constant, with value $1.7\times10^{-10}$ esu.

According to Tichý *et al* [78], nonlinear refractive index can be calculated according to the following equations.

$$n_2 = \frac{12\pi\chi^{(3)}}{n_o} \tag{31}$$

From table 6, it can be seen that the values of $\chi^{(3)}$ has increased from $2.55 \times 10^{-16}$ esu for the composite sample with FL 0.0 wt% to $11059.1 \times 10^{-16}$ esu for the composite sample with FL 4.89 wt%. This result shows an enhancement in the nonlinear optical characteristics of the material on incorporating the $TiO_2$ NPs. This may be due to the decreased gap between the electronic states due to introduction of new electronic states (associated with $TiO_2$ NPs). This results in the enhancement of susceptibility magnitudes.

## 4. Conclusions

$TiO_2$ NP-filled PVA/Ac–PVP polymer composites were prepared by solution casting technique. SEM images were helpful to study the variation in the surface morphology. EDS spectra of these composites were used to determine the constituent elements present in the samples. The effect of incorporating $TiO_2$ NPs on various linear and nonlinear optical parameters of $TiO_2$ NP-filled PVA/Ac–PVP polymer composites was studied in detail. The optical bandgap decreases with the increase in $TiO_2$ NP concentration in the PVA/Ac–PVP blend matrix. Refractive index of the composite increases with the increase in FL. Although the real and imaginary parts of dielectric constant for $TiO_2$ NP-filled PVA/Ac–PVP polymer composites exhibited the same nature, the values of $\varepsilon_1$ were found to be greater than $\varepsilon_2$. Volume and surface energy loss functions (VELF and SELF) increased with an increase in FL. The Wemple and DiDomenico model was used to obtain various dispersive parameters. The parameters, such as $E_d$, $f$, $n_o$, $M_{-1}$, $M_{-3}$, $N/m*$, $\omega_p$, $\lambda_o$, $S_o$, $E_o$ were determined. The values of high energy dielectric constant ($\varepsilon_\infty$) was determined from two different methods, and the values obtained were comparable with each other. Nonlinear optical parameters such as $\chi^{(1)}$, $\chi^{(3)}$ and $n_2$ were determined, and their values increased with an increase in FL. It can be seen that the values of linear and nonlinear parameters of $TiO_2$ NP-filled PVA/Ac–PVP polymer composites increased with an increase in the FL. Thus, $TiO_2$-filled PVA/Ac–PVP can be considered as a promising material for flexible optoelectronic applications.

## Acknowledgements

The facilities at the University Science Instrument Centre (USIC) and DST-SAIF, Karnatak University, Dharwad (KUD), have been used for recording UV/VIS spectra. We acknowledge that the SEM images along with EDS spectra were recorded at the Indian Institute of Technology (IIT), Kanpur. Veena acknowledges the receipt of RGNF from UGC, Government of India. The funding was provided by University Grants Commission (Grant No. 2016-17/RGNF-2015-17-SC-KAR-22364).

## References

[1] Zidan H M, Abdelrazek E M, Abdelghany A M and Tarabiah A E 2019 *J. Mater. Res. Technol.* **8** 904
[2] Meyer W H 1998 *Adv. Mater.* **10** 439
[3] Abdelrazek E M, Asnag G M, Oraby A H, Abdelghany A M, Alshehari A M and Gumaan M S 2020 *J. Electron. Mater.* **49** 6107
[4] Mohan V M, Bhargav P B, Raja V, Sharma A K and Rao V V R N 2007 *Soft Mater.* **5** 33
[5] Ngai K S, Ramesh S, Ramesh K and Juan J C 2016 *Ionics* **22** 1259
[6] Cardona M (ed) 1983 *Light scattering in solids I* (Berlin, Germany: Springer)
[7] Träger F (ed) 2012 *Springer handbook of lasers and optics* (New York: Springer)
[8] Bower D I 1997 in I M Ward (ed) *Structure and properties of oriented polymers* (Dordrecht: Springer) p 181
[9] Baraker B M 2017 Ph.D. Thesis, Karnatak University, Dharwad

[10] Ali F M and Kershi R M 2020 *J. Mater. Sci. Mater. Electron.* **31** 2557
[11] Badawi A 2020 *Appl. Phys. A* **126** 335
[12] Hadi A, Hashim A and Al-Khafaji Y 2020 *Trans. Electr. Electron. Mater.* **21** 283
[13] Jebur Q M, Hashim A and Habeeb M A 2019 *Trans. Electr. Electron. Mater.* **20** 334
[14] Sengwa R J and Dhatarwal P 2021 *Opt. Mater.* **113** 110837
[15] Fischer H 2003 *Mater. Sci. Eng. C* **23** 763
[16] Abdelghany A M, Farea M O and Oraby A H 2021 *J. Mater. Sci. Mater. Electron.* **32** 6538
[17] Hema S and Sambhudevan S 2021 *Chem. Pap.* **75** 3697
[18] El Sayed S and Sayed A M E 2021 *J. Mater. Sci.: Mater. Electron.* **32** 13719
[19] Turky G and Dawy M 2003 *Mater. Chem. Phys.* **77** 48
[20] Venkatachalam S 2016 *Spectroscopy of polymer nanocomposites* (Norwich, UK: William Andrew Publishing) p 130
[21] Stepanov A L 2019 in Pielichowski K and Majka T M (eds) *Polymer composites with functionalized nanoparticles* (Netherlands: Elsevier) p 325
[22] Soliman T S and Vshivkov S A 2019 *J. Non-Cryst. Solids* **519** 119452
[23] Kulyk B, Essaidi Z, Luc J, Sofiani Z, Boudebs G, Sahraoui B *et al* 2007 *J. Appl. Phys.* **102** 113113
[24] Abdullah O G, Aziz S B, Omer K M and Salih Y M 2015 *J. Mater. Sci. Mater. Electron.* **26** 5303
[25] Iliopoulos K, Kasprowicz D, Majchrowski A, Michalski E, Gindre D and Sahraoui B 2013 *Appl. Phys. Lett.* **103** 231103
[26] Caseri W 2008 *Chem. Eng. Commun. C* **196** 549
[27] Wilson J L, Poddar P, Frey N A, Srikanth H, Mohomed K, Harmon J P *et al* 2004 *J. Appl. Phys.* **95** 1439
[28] Burke N A D, Stöver H D H and Dawson F P 2002 *Chem. Mater.* **14** 4752
[29] Fang J, Tung L D, Stokes K L, He J, Caruntu D, Zhou W L *et al* 2002 *J. Appl. Phys.* **91** 8816
[30] Lévy R, Shaheen U, Cesbron Y and Sée V 2010 *Nano Rev.* **1** 4889
[31] Lin M M, Kim H H, Kim H, Muhammed M and Kim D K 2010 *Nano Rev.* **1** 4883
[32] Abdullah O G, Tahir D A and Kadir K 2015 *J. Mater. Sci. Mater. Electron.* **26** 6939
[33] Abdelghany A M, Abdelrazek E M and Rashad D S 2014 *Spectrochim. Acta A* **130** 302
[34] Shetty B G, Crasta V and Rajesh K 2020 *AIP Conf. Proc.* **2269** 030092
[35] Devikala S, Kamaraj P and Arthanareeswari M 2013 *Int. Res. J. Pure Appl. Chem.* **3** 257
[36] Li S, Lin M M, Toprak M S, Kim D K and Muhammed M 2010 *Nano Rev.* **1** 5214
[37] Cheremisinoff N P 1997 *Handbook of engineering polymeric materials* (New York: Marcel Dekker Inc.)
[38] Lewis S, Haynes V, Wheeler-Jones R, Sly J, Perks R M and Piccirillo L 2010 *Thin Solid Films* **518** 2683
[39] Matilainen A and Sillanpää M 2010 *Chemosphere* **80** 351
[40] Wouters M, Rentrop C and Willemsen P 2010 *Prog. Org. Coat.* **68** 4
[41] Lewandowska K 2005 *Eur. Polym. J.* **41** 55
[42] Lobo B and Veena G 2021 *Polym-Plast. Technol. Mater.* **60** 1697
[43] Bhargav P B, Mohan V M, Sharma A K and Rao V V R N 2009 *Curr. Appl. Phys.* **9** 165
[44] Babu J R, Ravindhranath K and Vijaya Kumar K 2018 *Adv. Mater. Sci. Eng.* **2018** 1
[45] Abarna S and Hirankumar G 2019 *Mater. Sci.-Pol.* **37** 331
[46] Lee S, Koo B, Shin J, Lee E, Park H and Kim H 2006 *Appl. Phys. Lett.* **88** 162109
[47] Choi J S 2008 *J. Inf. Disp.* **9** 35
[48] Ramesan M T, Varghese M, Jayakrishnan P and Periyat P 2018 *Adv. Polym. Technol.* **37** 137
[49] Sudheesh P, Sharafudeen K N, Vijayakumar S and Chandrasekharan K 2011 *J. Opt.* **40** 193
[50] Shahenoor Basha S K and Rao M C 2018 *Polym. Sci. Ser. A* **60** 359
[51] Kumar S, Prajapati G K, Saroj A L and Gupta P N 2019 *Physica B* **554** 158
[52] Hirankumar G, Selvasekarapandian S, Kuwata N, Kawamura J and Hattori T 2005 *J. Power Sour.* **144** 262
[53] Abdelrazek E M 2007 *Physica B* **400** 26
[54] Tauc J 1974 (ed) *Optical properties of amorphous semiconductor* (London: Plenum Publishing Company Ltd) p 159
[55] Mott N F and Davis E A 1979 (eds) *Electronic processes in non-crystalline materials* (London: Oxford University Press) p 272
[56] Elashmawi I S, Abdelrazek E M, Ragab H M and Hakeem N A 2010 *Physica B* **405** 94
[57] Veena G and Lobo B 2021 *J. Phys. Condens. Matter* **33** 255101
[58] Abdel-Aziz M M, El-Metwally E G, Fadel M, Labib H H and Afifi M A 2001 *Thin Solid Films* **386** 99
[59] Tauc J, Grigorovici R and Vancu A 1966 *Phys. Status Solidi B* **15** 627
[60] Tikhonov E A, Ivashkin V A and Ljamec A K 2012 *J. Appl. Spectrosc.* **79** 148
[61] Tohyama T and Maekawa S 1991 *J. Phys. Soc. Jpn.* **60** 53
[62] Kaczmarek H and Podgórski A 2007 *J. Photochem. Photobiol. A* **191** 209
[63] Yakuphanoglu F, Cukurovali A and Yilmaz I 2004 *Physica B* **351** 53
[64] Hafiz M M, Mahfoz Kotb H, Dabban M A and Abdel-latif A Y 2013 *Opt. Laser Techol.* **49** 188
[65] Wemple S H and Didomenico M 1971 *Phys. Rev. B* **3** 1338
[66] Wemple S H 1973 *Phys. Rev. B* **7** 3767
[67] DrDomenico Jr. M and Wemple S H 1969 *J. Appl. Phys.* **40** 720
[68] Abdullah O G, Salh D M, Mohamad A H, Jamal G M, Hawzhin T A, Bakhan S M *et al* 2021 *J. Electron. Mater.* **51** 675
[69] Mohamad A H, Saeed S R and Abdullah O G 2019 *Mater. Res. Express* **6** 115332
[70] Wemple S H and DiDomenico M 1969 *Phys. Rev. Lett.* **23** 1156
[71] O'Leary S K, Zukotynski S and Perz J M 1997 *J. Non-Cryst. Solids* **210** 249
[72] Omar M A 2006 *Elementary solid state physics* (England: Pearson Education Inc.) p 372
[73] Baleva M, Goranova E, Darakchieva V, Kossionides S, Kokkosis M and Jordanov P 2002 *Vacuum* **69** 425
[74] Moss T S 1959 in Hogarth C A (ed) *Optical properties of semiconductors* (London: Butterworth Scientific Publications Ltd)

[75] Zemel J N, Jensen J D and Schoolar R B 1965 *Phys. Rev.* **140** A330
[76] Soliman T S, Vshivkov S A and Elkalashy Sh I 2020 *Opt. Mater.* **107** 110037
[77] Abomostafa H M 2021 *J. Mol. Struct.* **1225** 129126
[78] Tichý L, Tichá H, Nagels P, Callaerts R, Mertens R and Vlček M 1999 *Mater. Lett.* **39** 122
[79] Gupta V and Mansingh A I 1996 *J. Appl. Phys.* **80** 1063
[80] Gad S A and Moez A A 2020 *J. Inorg. Organomet. Polym. Mater.* **30** 469